Proceedings of the Sixth International Conference on
Railway Technology: Research, Development and Maintenance
Edited by: J. Pombo
Civil-Comp Conferences, Volume 7, Paper 3.20
Civil-Comp Press, Edinburgh, United Kingdom, 2024
ISSN: 2753-3239, doi: 10.4203/ccc.7.3.20
©Civil-Comp Ltd, Edinburgh, UK, 2024

Aerodynamics of Freight Trains: An Open Database of Geometries for CFD Analyses

L. Corniani, P. Schito and S. Bruni

**Department of Mechanical Engineering, Politecnico di Milano
Italy**

Abstract

The computational investigation of freight train aerodynamics requires the production of a surface geometry of the vehicle in order to run the simulation. To address the need for efficient production of these geometries that comes with the growing employment of numerical studies in this field, a database of representative wagon and locomotive geometries is proposed in this work.
After the database is introduced, a demonstrational computational fluid dynamics study is presented, considering the geometry of a single flat wagon with a container for two different levels of detail, and the results of the simulations are compared and discussed.

Keywords: train aerodynamics, freight trains, database, container, computational fluid dynamics, URANS.

1 Introduction

The strategic European goal to shift the long-distance-transport of goods from road to rail necessitates the eventual increase in the speed of freight trains to at least 160 km/h (Geischberger et al. [1]). At this speed, the aerodynamic effects that are mostly negligible at lower speeds become highly relevant.

Aerodynamic forces grow approximately with the square of the velocity of the flow, thus increasing the train speed resulting in greater aerodynamic forces on the vehicle. Research from Quazi et al. [2] and Alam et al. [3] shows that freight trains encounter wind from yaw angles mostly below 20°, and therefore the main component of the aerodynamic force on a moving train is drag. This means that the increase of service speed has direct consequences for the cost and environmental impact of the operation of the train, since the mechanical power spent by the locomotive is proportional to the overall resistance to motion. Other components of the force are also of interest, since both lift and side force generate overturning moment on the wagons and must be contained to reduce the risk of derailment.

A subject of intense study directly linked to drag is the effect of empty wagons and of the size of gaps between containers, Maleki et al. [4] showed that the pressure component of drag is closely related to the size of the gap between containers. Additionally, slipstream velocities generated by a freight train tend to increase for larger gaps (Flynn et al. [5] and Li et al. [6]), in the absence of crosswind, these velocities are not sufficient to put a person stability at risk, but crosswind amplifies this effect enough to destabilize large portions of the population (Flynn et al. [7]).

Unlike streamlined passenger trains, freight trains behave as bluff-bodies and thus the flow around these vehicles is more turbulent and intrinsically unsteady. The study of freight train aerodynamics is further complicated by the fact that they can be composed of a variety of wagons with diverse geometries. These differences between passenger and freight trains call for an investigation of the flow around the latter as a separate endeavour.

The aerodynamics of freight train has been studied in the literature with both numerical and experimental methods, complementing each other with their relative strengths and drawbacks. Experimental methods measure pressure and flow velocity directly and therefore are inherently more reliable than numerical methods, however, they are also much more expensive and time-consuming.

Most experimental studies on freight trains are conducted in wind tunnels. Alam et al. [8] performed a wind tunnel test on a 1:15 model scale of a double stacked container wagon in isolation; subsequent studies by Giappino et al. [9], Kocon et al. [10] and Alam et al. [3] focused on the risk of overturning caused by crosswind on freight wagons and concluded that the relative aerodynamic coefficients are larger at high yaw angles (although a train is unlikely to encounter such angles while in motion). Wind tunnel tests have also been used by Soper et al. [11] and Sterling et al. [12] to study the slipstream velocities generated by freight trains and found them to be much greater than what was observed in passenger trains. Intermodal transport of freight has also been the subject of wind tunnel tests. Giappino et al. [13] tested different train configurations with different gap sizes and concluded that for each wagon, the best condition (both in terms of drag and overturning moments) is to be preceded by a loaded wagon and followed by an empty one. This is true for the single wagon, however, whilst for the purpose of minimizing the drag for the entire train smaller gap sizes are to be preferred, as shown based on wind tunnel tests by Soper et al. [14] and on CFD by Maleky et al. [4].

In all wind tunnel experiments that involve freight trains, the Reynolds number of the test is much lower than in full-scale experiments and this makes the latter more reliable, however the former is still often preferred for the lower costs also considering that for Reynolds numbers greater than $2.5 \cdot 10^5$ the aerodynamic coefficients become insensitive to Reynolds number (Bocciolone et al. [15]). Soper et al. [16] used full-scale experiments to compare the aerodynamics of passenger and freight trains and found that freight trains at low speed generate slipstream velocities higher than the passenger trains, although not in violation of the TSI regulations (it should however be noticed that numerical investigations by Flynn et al. [7] found that in cases of crosswinds at a yaw angle of 30° the slipstream velocities produced by freight trains even at moderate velocities were in violation of the TSI limits for faster trains). The measurement of a full-scale underbody flow has been used by Soper et al. [17] to conclude that on well-maintained tracks the aerodynamic forces on ballast and the inertial ones due to track displacement are comparable, but poorly maintained tracks may increase the risk of ballast flight significantly.

Numerical studies allow to evaluate the flow in every point of the domain; however, the results are also affected by the physical modelling of the problem, and one of the most significant decisions to make in CFD is the modelling method for turbulence.

Different works have been published comparing the accuracy and cost of different methods (Wang et al. [18], Wang et al. [19] and Maleki et al. [20]) and they agree on the fact that RANS and URANS are unsuitable for the simulation of freight trains because of the pronounced unsteadiness of the flow. The expensive LES (or more often in recent works ELES, DES or DDES) are generally agreed to be the most accurate methods, predicting flow topology and aerodynamic coefficients in line with experimental results. It should be noted however, that while RANS methods fail to predict the numerical value of aerodynamic coefficients, they predict their trends and are suitable for comparing the performance of different geometries (Maleki et al. [20]).

The Academics4Rail research project, funded by the European community under the Europe's Rail funding programme, has launched a comprehensive investigation on the aerodynamics of freight trains. The objective is to define guidelines for the creation of CFD models of freight trains, analyse different realistic operation scenarios and synthesise the results in guidelines for safer and more efficient operation of freight trains in regard of aerodynamic effects.

Given the breadth of the problems addressed, the need for the efficient definition of geometric models for single vehicles (locomotives and wagons) and for complete freight trains becomes apparent. Therefore, a first part of the research is devoted to creating a database of geometries for vehicles and vehicle parts in formats that are compatible with software for CFD simulation. In this way, complex geometries representative of realistic freight operation scenarios can be efficiently created. In the creation of the database, a defeaturing process is applied and vehicle geometries are defined at different levels of detail, allowing the efficient creation of simpler and more detailed CFD models, in view of finding a trade-off between accuracy and computational efficiency.

This paper presents some initial results from the research. In particular, defnition of the geometry database is presented, then the results of a CFD analysis of a single freight wagon is presented, comparing the results for different levels of detail of vehicle geometry.

The paper is structured as follows: in section 2 of the paper a detailed description of the geometries and the process by which they have been created and stored in the database is provided. In section 3 an exemplary CFD analysis is presented, analysing the mesh independence and a comparison between levels of detail. Finally, in section 4 conclusion and final remarks are drawn.

2 The database of freight train geometries

Unlike passenger trains, freight trains exhibit a wide variety of geometries both because of the diversity of the wagons that make them up and because of the many different compositions (what type of wagons they are made of, and in what order) that they can have.

The study of the aerodynamics around these vehicles therefore is only possible if an efficient and versatile method for producing diverse freight train geometries is developed. The aim of the database proposed in this work is to address this need while allowing the user to balance between higher levels of detail and computational cost.

Before the construction of the database could begin, a classification of locomotives and wagon types was necessary. While no official classification exists, freight wagons can be broadly distinguished according to these categories: Open wagons, Covered wagons, Flat wagons, Dump cars, High-capacity wagons, Special wagons, and Tank wagons. Although this way of distinguishing freight wagons has been also adopted with minor variations elsewhere in literature, these specific categories have been taken from Principe [21]. Locomotives are more homogenous in their geometry, so they have not been classified in a similar way, instead three versions meant to resemble slight variations in existing locomotives are proposed. Finally, each of the geometries are provided in different levels of detail. The classification is showcased in Figure 1.

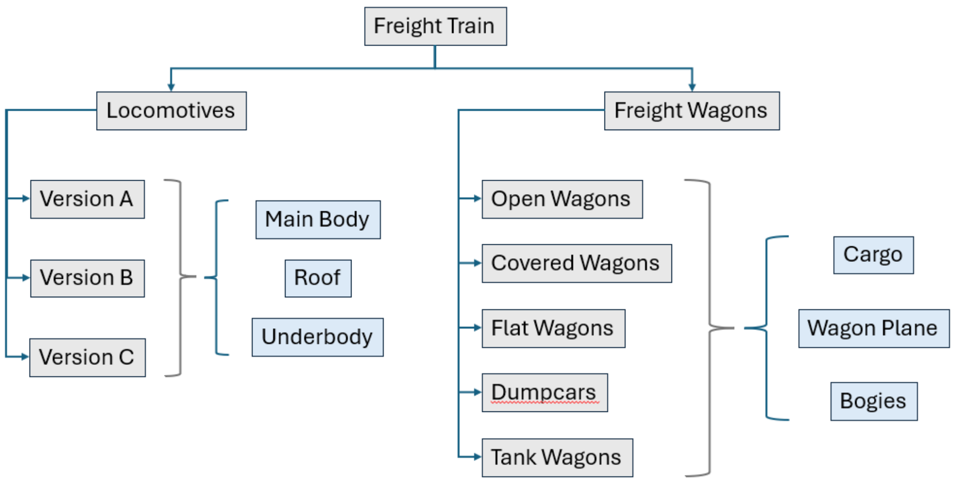

Figure 1: Classification of the database.

A modular approach is used to build the geometric models of the vehicles. All wagons are composed of three parts: a wagon plane, bogies, and cargo (where cargo refers to the geometry above the wagon plane, this is the distinguishing part of each category of wagon). In Figure 2, the components of tank wagons are shown, the cargo of course will be different for other categories of wagon, Figure 3 shows the version B of the locomotive in its three components.

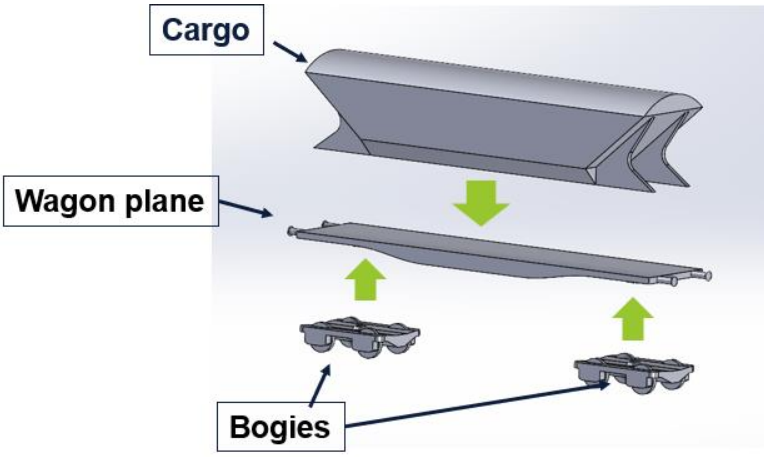

Figure 2: All wagon components.

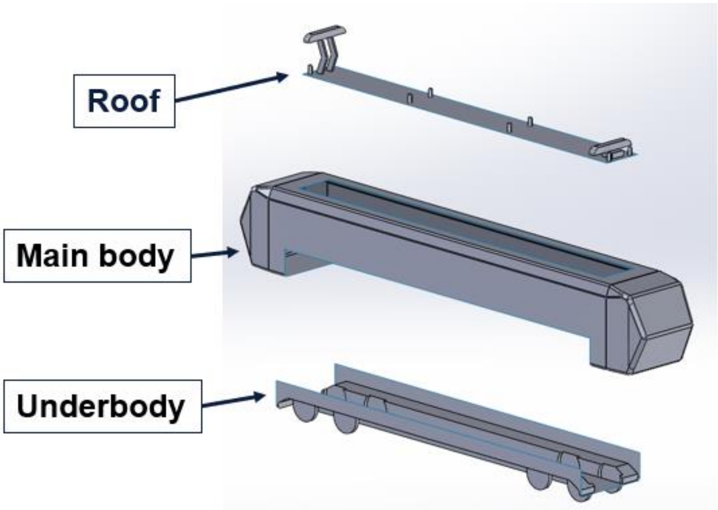

Figure 3: All components of locomotives, version B.

The database consists of the assembled geometries together with the modular parts that make them up, therefore every user will have access to the geometries of all components of the vehicles. The main advantage of structuring the database with this modular approach is that it allows the user to select the level of detail of each component and, to a degree, customize the geometry based on their necessity. Additionally, the geometries built with the same components allow to properly compare the effect of the cargo on the flow around the vehicle, while if all models were subtly different the effect of the intended and unintended differences would be confounded. As a final advantage, this approach allows for faster production and update of geometries.

The database includes geometries of both locomotives and wagons, the locomotives are made of three parts: the main body, the underbody, and the roof. What differentiates one locomotive version from another is the main body, since the underbody and roof are designed so as to be interchangeable.

The design of the main bodies for all locomotive versions followed the same workflow: first, a basic structure is defined through the use of a certain number of parameters as shown in Figure 4, then the volume enclosed in the structure is extruded and the edges are rounded (with the radii being parametrically defined as well), and finally, the surface of the main body is obtained from the volume.

The surface obtained is at this point a closed surface, to complete the geometry it needs to be trimmed along well-defined curves. The final result is an open surface with boundaries that match those of other components of the locomotive, so that when they are all assembled, they constitute a closed surface again. Figure 5 shows the main body of the version C of the locomotive. It is worth noting that all locomotive geometries are symmetrical with respect to a plane normal to the direction of motion, therefore no additional information would be gained by reporting the entire geometry in a figure.

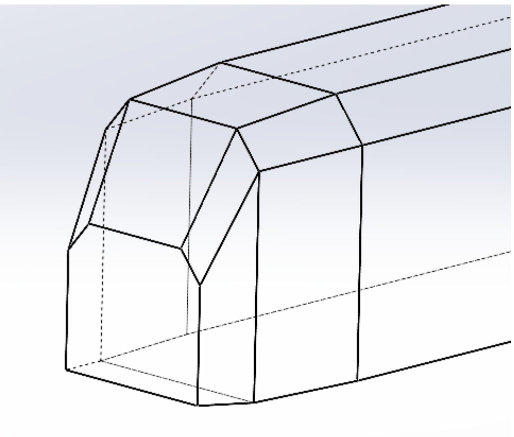

Figure 4: Structure of the locomotive, version C.

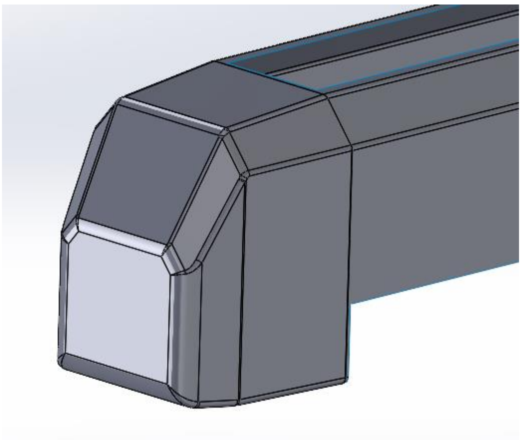

Figure 5: Main body component of the locomotive, version C.

Roof and underbody geometries in real locomotives are very different from model to model, therefore modelling a general version of these geometries is a summary endeavour by necessity, however, some parts of these geometries are standardized. In the making of the roof geometries, pantographs are surely a prominent feature, therefore they have been modelled to resemble the actual dimensions reported by Baker et al. [22]. Figure 6 shows the roof geometries, from left to right in increasing level of detail.

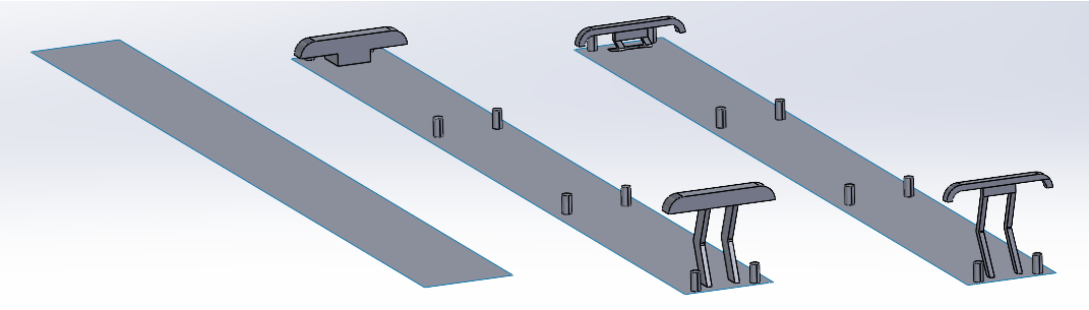

Figure 6: From left to right: Roof component, least detailed version; roof component, medium detailed version; roof component, more detailed version.

The final component of the locomotive geometry is the underbody. Similarly to the roof, the underbody geometries of actual locomotives are very diverse, and so the same strategy has been adopted; the dimensions of standardized parts have been taken from Principe [21] to make the geometry broadly realistic. Figure 7 and Figure 8 show respectively the underbody components (in increasing order of detail from left to right as before) and the complete (assembled) locomotive geometry.

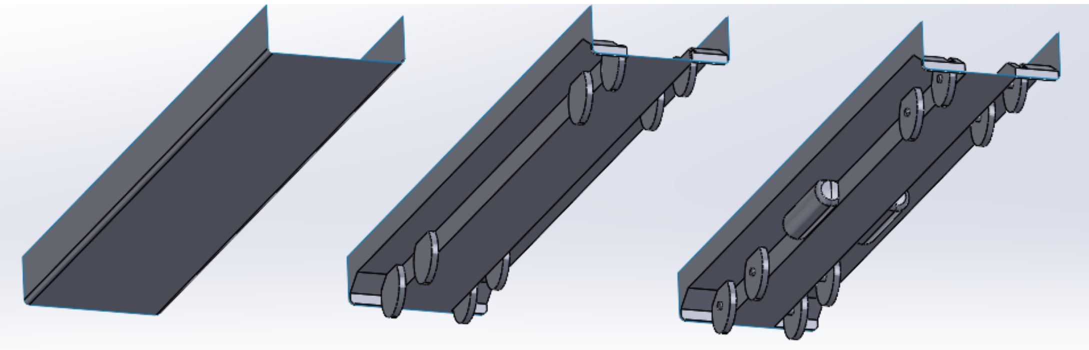

Figure 7: From left to right: Underbody component, least detailed version; underbody component, medium component version; underbody component, most detailed version.

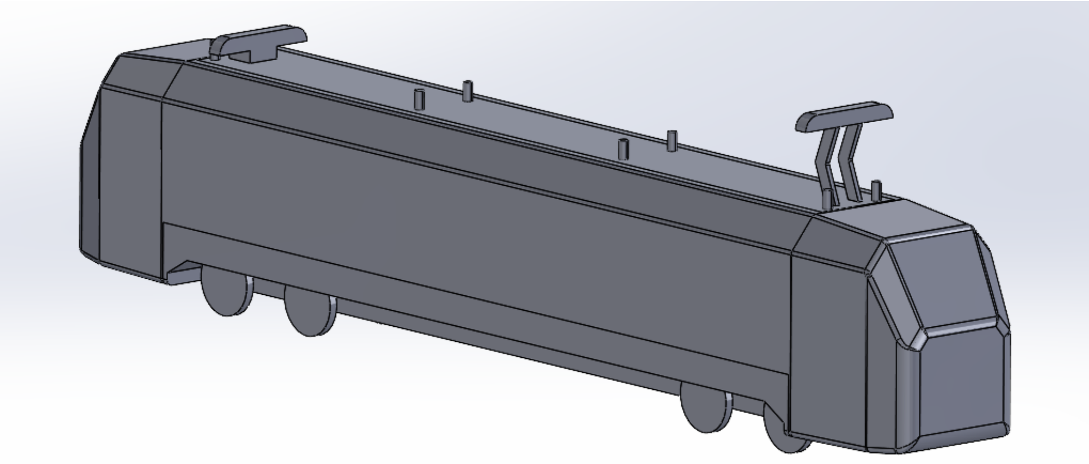

Figure 8: Assembled locomotive, version C, medium level of detail.

Like for other parts, the geometries of the roof and underbody components underwent a defeaturing process to produce the different levels of detail displayed in Figure 6 and Figure 7. The removal of details is always aimed at simplifying the mesh without sacrificing accuracy, thus the defeaturing process was carried out by removing those detail that were deemed to need a more complex profile while having little impact on the overall flow. As a general rule, features that changed the front area of the geometry were deemed more impactful on the flow than features that did not, so the former were removed only in the last iterations of defeaturing, and the latter were removed immediately. Similarly, the more voluminous features were deemed more impactful on the flow than smaller ones.

The geometry of the wagons is comprised of three components as shown in Figure 2, two of which are the same for all wagon types, for reasons already mentioned, the components referred to as bogies and plane in Figure 2 have been kept the same for all wagons, whereas the component referred to as cargo changes for the different types. However, it should be noticed that not all wagon types have a cargo, indeed flat wagons may carry one container, two container, or be empty, in the latter case the wagon is composed by plane and bogies alone.

All wagon components have been designed as closed surfaces and feature planar faces that act as interface between components. This means that all components at all levels of detail must be present planar surfaces in the right places to allow for the faces to overlap in one interface. Figure 9 shows in red the interfaces between bogies and plane and in green the one between plane and cargo.

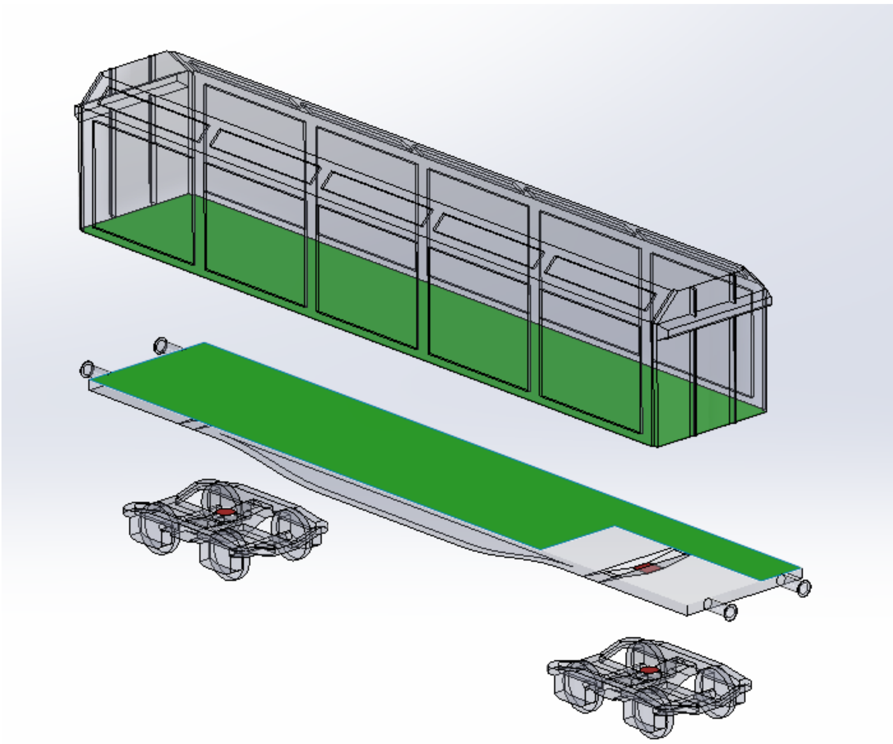

Figure 9: Components of a covered wagon with its interface surfaces highlighted.

The modelling process of the bogies was carried out using an actual 3D model of the Y25 bogies, therefore the first version of the component (see Figure 10) was the most detailed one, the less detailed versions were obtained after successive defeaturing iterations following the same criteria as outlined previously. The other components have been realized without 3D models; therefore, the opposite workflow was adopted. The simpler version was made first in such a way as to resemble the most important aerodynamic features of the commercially available models, and then more and more detailed versions were obtained as modified versions of the first one. As an example, Figure 11 shows the wagon plane in its levels of detail.
With all of the components modelled, the last step consisted in assembling and uploading the files to a public GitHub repository, available here. All the geometries have been uploaded in step format and are available both as preassembled single vehicles (the assemblies have only been made with components with consistent level of detail), and single components (available at all levels of detail).

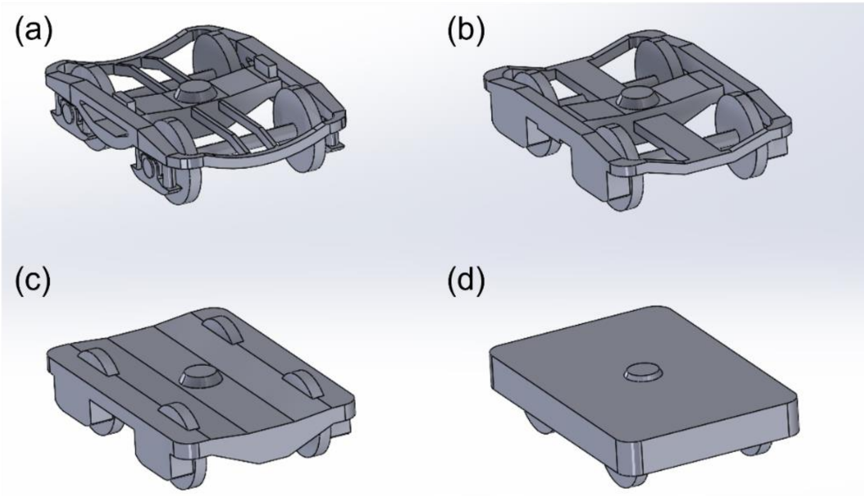

Figure 10: Bogies components in different levels of detail: (a) Most detailed; (b) More detailed; (c) Medium detailed; (d) Less detailed.

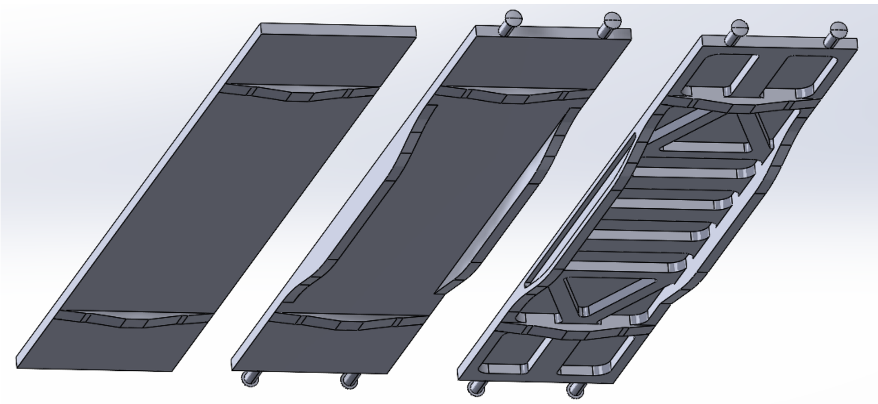

Figure 11: From left to right: wagon plane, least detailed; wagon plane, medium detailed; wagon plane, most detailed.

The database presented in this work can be used for the simulation of the aerodynamics of a generic freight train, but further improvements are possible. One possibility is the addition of more geometries, for example geometries for double stacked containers can be added to the cargo components, longer versions of some wagon types could be considered (for example, the covered wagons and the flat wagons are sometimes designed with longer planes for greater capacity), and some special purpose wagons could be added as well. Another way of improving on the present work would be to simplify the process of composing a train of chosen composition, a software to manipulate the coordinates within the files would be the most suitable tool for this.

3 CFD analysis of single wagon

In this section, the simple case of a single flat wagon with a 40 ft container moving at 160 kmh^{-1} in steady air is considered.

The simulations have been carried out using the open-source software OpenFoam v10, the solution was achieved in two steps: the first consisted in the evaluation of the steady state flow, and the second one in the calculation of the unsteady flow using the steady solution as a starting point for the simulation. The steady state simulation was carried out with the SIMPLE algorithm starting from the solution of the potential flow, the linear scheme was used for the gradient of velocity and the upwind scheme for its divergence. The k-ω SST turbulence model was adopted for both steady-state and transient runs. The unsteady simulations were carried out with the PIMPLE algorithm, using the solution from the steady one as initial conditions with the same settings as before (except of course for the time-derivative, for which the implicit Euler scheme was chosen).

Figure 12 shows the domain dimensions in terms of lengths (L), widths (W) and heights (H) of the wagon, a zero-gradient boundary condition was chosen for pressure for the ground and wagon patches, with no-slip condition for the velocity. The inlet velocity was set to 160 kmh^{-1} and at the outlet pressure a zero-gradient was imposed, zero-gradient for pressure and slip condition for velocity were set on all remaining patches.

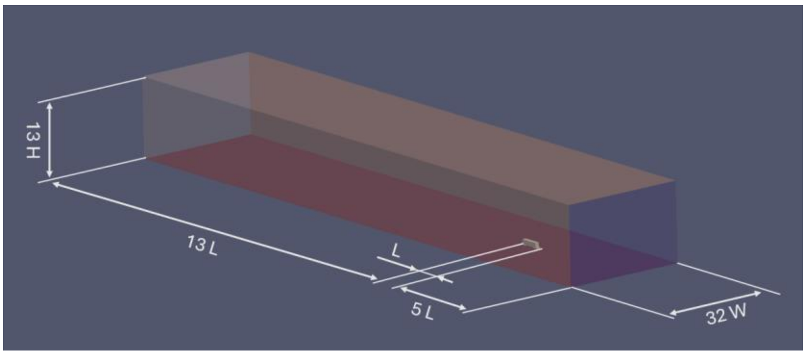

Figure 12: Simulation domain.

The meshes were all structured and have been obtained with the inbuilt OpenFoam application snappyHexMesh, with a refined region around the wagon.

For the simulations of the flow around the proposed geometries to be useful, they have at least to be independent of the grid, thus a convergence study was carried out. Table 1 reports the aerodynamic coefficients for lift and drag determined with meshes of different level of refinement in a steady-state simulations. The coefficients have been calculated using a reference area of 10 m^2 according to expressions (1).

$$C_D = \frac{2D}{\rho A {U_f}^2} \qquad C_L = \frac{2L}{\rho A {U_f}^2} \qquad C_S = \frac{2S}{\rho A {U_f}^2} \tag{1}$$

Where *D* is the pressure drag, *L* is the pressure lift, *S* is the pressure side force, ρ is the density of the air, *A* is the reference area and U_f is the freestream velocity of the air (44.44 ms^{-1})
Table 1 shows that the variations of aerodynamic coefficients remain below 1% beyond the 11.9 million cells grid, thus the results are deemed to be mesh independent beyond this level of refinement. It should be noted that, although the results remain consistent, they are numerically different from other findings in literature (Östh et al. [23]). This can be explained by the fact that the flow around freight wagons is strongly unsteady, therefore the steady-state solver should not be expected to accurately predict the value of the aerodynamic forces. This is a well know limitation of the RANS method that has been reported in the literature before by Maleki et al. [20], this method remains capable of predicting trends in aerodynamic forces and is useful for comparative investigations.

Number of cells [millions]	C_D [-]	C_L [-]	$\Delta C_D/C_D$ [%]	$\Delta C_L/C_L$ [%]
2.9	0.809	-0.207	+0.24%	-6.94%
4.4	0.811	-0.192	+0.44%	+5.84%
6.3	0.814	-0.204	+0.65%	+8.04%
8.9	0.819	-0.220	-0.06%	+1.08%
11.9	0.819	-0.222	-0.53%	-0.63%
15.6	0.815	-0.221	+0.59%	-0.44%
20.1	0.819	-0.220		

Table 1: Convergence of aerodynamic coefficients for with different grids

The URANS method, although unsteady, has been reported to be unsuitable to evaluate accurately the aerodynamic forces on a vehicle as if fails to correctly predict the length of recirculation regions (Wang et al. [18] and Maleki et al. [20]), but despite this limitation, the unsteady simulations run in this work have produced a significant improvement in the accuracy of the aerodynamic coefficients. Table 2 shows the results for force coefficients averaged over the last 5 seconds of the run for the less-detailed version and medium-detailed version of the wagon as defined in expression (1). The drag coefficients are comparable to those obtained with LES by Östh et al. [23], while the lift remains overpredicted. Finally, Figure 13 shows the magnitude velocity field on the xz-plane and Figure 14 shows the longitudinal velocity profiles on top of the container in correspondence to the white lines indicated in Figure 13, which demonstrate that the simulation captured the recirculation of the flow.

	C_D [-]	C_L [-]	C_S [-]
Less detailed wagon	0.862	-0.218	0.011
Medium detailed wagon	0.878	-0.170	0.006

Table 2: Time-averaged aerodynamic coefficients from unsteady simulations.

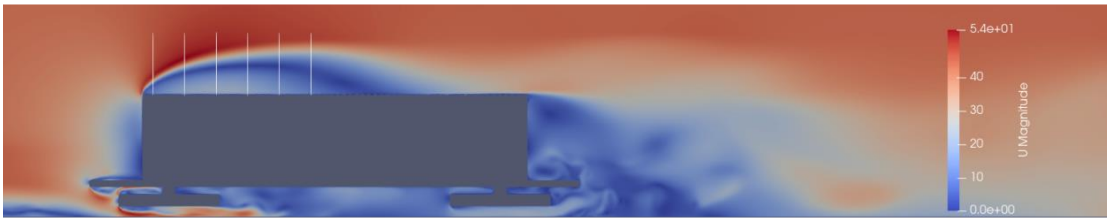

Figure 13: Magnitude velocity field of the unsteady simulation of the medium detailed geometry.

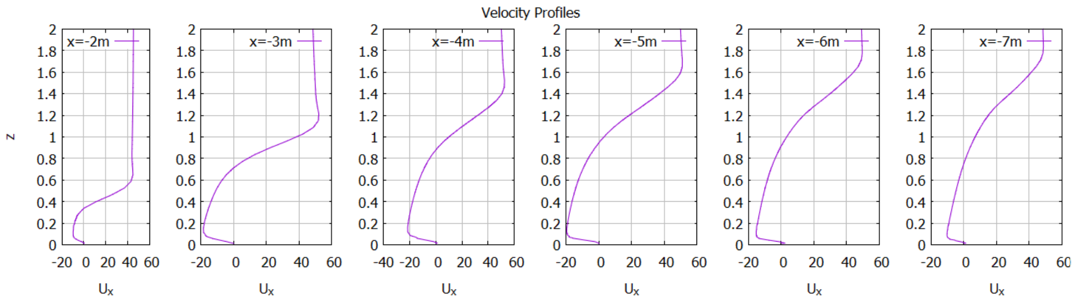

Figure 14: Profiles of the x component of the velocity on top of the container.

4 Conclusions and Contributions

In this work, a database for the efficient production of surface geometries for the CFD simulations of freight trains has been proposed, and some demonstrational steady and transient simulations have been run on the geometry of a container wagon at a lesser and higher level of detail. The database allows for the user to choose between different types of wagons, and to compose the wagon with individual components. In this way the user can form a single wagon or an entire train with components having different levels of detail in different parts, allowing for the efficient production of customized freight trains geometries.

With proper grids, the steady simulations reached consistent results for aerodynamic force coefficients but failed to replicate the more accurate results obtained in literature with methods better suited for unsteady flows; in particular, they underpredicted the drag and overpredicted the lift. The failure of the RANS method to accurately evaluate aerodynamic forces on the vehicle is explained by its inability to capture the markedly unsteady nature of the flow, with the result of obtaining a non-physical solution. A significant improvement was provided by the URANS simulations which managed to reproduce results for the drag well comparable with more accurate methods (discrepancies with LES within 5%), although with overprediction of the lift. Additionally, the unsteady method managed to capture the recirculation region on top of the container near the leading edge.

Acknowledgements

The research reported in this paper has received funding from the European Union's Horizon Europe research and innovation programme under grant agreement: HORIZON-ER-JU-2022-ExplR-04. Views and opinions expressed are however those of the authors only and do not necessarily reflect those of the European Union or Europe's Rail Joint Undertaking. Neither the European Union nor the granting authority can be held responsible for them.

References

[1] J. Geischberger and M. Moensters, "Impact of faster freight trains on railway capacity and operational quality," *International Journal of Transport Development and Integration*, vol. 4, no. 3, pp. 274–285, Jul. 2020, doi: 10.2495/TDI-V4-N3-274-285.

[2] A. Quazi, T. Crouch, J. Bell, T. McGreevy, M. C. Thompson, and D. Burton, "A field study on the aerodynamics of freight trains with different stacking configurations," *Journal of Wind Engineering and Industrial Aerodynamics*, vol. 232, Jan. 2023, doi: 10.1016/j.jweia.2022.105245.

[3] F. Alam and S. Watkins, "Lateral stability of a double stacked container wagon under crosswind," *Proceedings of the International Conference on Mechanical Engineering 2007*, 2007.

[4] S. Maleki, D. Burton, and M. C. Thompson, "Flow structure between freight train containers with implications for aerodynamic drag," *Journal of Wind Engineering and Industrial Aerodynamics*, vol. 188, pp. 194–206, May 2019, doi: 10.1016/j.jweia.2019.02.007.

[5] D. Flynn, H. Hemida, D. Soper, and C. Baker, "Detached-eddy simulation of the slipstream of an operational freight train," *Journal of Wind Engineering and Industrial Aerodynamics*, vol. 132, pp. 1–12, 2014, doi: 10.1016/j.jweia.2014.06.016.

[6] C. Li, D. Burton, M. Kost, J. Sheridan, and M. C. Thompson, "Flow topology of a container train wagon subjected to varying local loading configurations," *Journal of Wind Engineering and Industrial Aerodynamics*, vol. 169, pp. 12–29, Oct. 2017, doi: 10.1016/j.jweia.2017.06.011.

[7] D. Flynn, H. Hemida, and C. Baker, "On the effect of crosswinds on the slipstream of a freight train and associated effects," *Journal of Wind Engineering and Industrial Aerodynamics*, vol. 156, pp. 14–28, Sep. 2016, doi: 10.1016/j.jweia.2016.07.001.

[8] F. Alam and S. Watkins, "Effects of Crosswinds on Double Stacked Container Wagons," Gold Coast, Australia, Dec. 2007.

[9] S. Giappino, D. Rocchi, P. Schito, and G. Tomasini, "Cross wind and rollover risk on lightweight railway vehicles," *Journal of Wind Engineering and Industrial Aerodynamics*, vol. 153, pp. 106–112, Jun. 2016, doi: 10.1016/j.jweia.2016.03.013.

[10] A. Kocoń and A. Flaga, "Critical velocity measurements of freight railway vehicles roll-over in wind tunnel tests as the method to assess their safety at

strong cross winds," in *Journal of Wind Engineering and Industrial Aerodynamics*, Elsevier B.V., Apr. 2021. doi: 10.1016/j.jweia.2021.104559.
[11] D. Soper, C. Baker, and M. Sterling, "Experimental investigation of the slipstream development around a container freight train using a moving model facility," *Journal of Wind Engineering and Industrial Aerodynamics*, vol. 135, pp. 105–117, Dec. 2014, doi: 10.1016/j.jweia.2014.10.001.
[12] M. Sterling, C. J. Baker, S. C. Jordan, and T. Johnson, "A study of the slipstreams of high-speed passenger trains and freight trains," *Proc Inst Mech Eng F J Rail Rapid Transit*, vol. 222, no. 2, pp. 177–193, 2008, doi: 10.1243/09544097JRRT133.
[13] S. Giappino, S. Melzi, and G. Tomasini, "High-speed freight trains for intermodal transportation: Wind tunnel study on the aerodynamic coefficients of container wagons," *Journal of Wind Engineering and Industrial Aerodynamics*, vol. 175, pp. 111–119, Apr. 2018, doi: 10.1016/j.jweia.2018.01.047.
[14] D. Soper, C. Baker, and M. Sterling, "An experimental investigation to assess the influence of container loading configuration on the effects of a crosswind on a container freight train," *Journal of Wind Engineering and Industrial Aerodynamics*, vol. 145, pp. 304–317, 2015, doi: 10.1016/j.jweia.2015.03.002.
[15] M. Bocciolone, F. Cheli, R. Corradi, S. Muggiasca, and G. Tomasini, "Crosswind action on rail vehicles: Wind tunnel experimental analyses," *Journal of Wind Engineering and Industrial Aerodynamics*, vol. 96, no. 5, pp. 584–610, May 2008, doi: 10.1016/j.jweia.2008.02.030.
[16] D. Soper and C. Baker, "A full-scale experimental investigation of passenger and freight train aerodynamics," *Proc Inst Mech Eng F J Rail Rapid Transit*, vol. 234, no. 5, pp. 482–497, May 2020, doi: 10.1177/0954409719844431.
[17] D. Soper *et al.*, "Full scale measurements of train underbody flows and track forces," *Journal of Wind Engineering and Industrial Aerodynamics*, vol. 169, pp. 251–264, Oct. 2017, doi: 10.1016/j.jweia.2017.07.023.
[18] S. Wang, J. R. Bell, D. Burton, A. H. Herbst, J. Sheridan, and M. C. Thompson, "The performance of different turbulence models (URANS, SAS and DES) for predicting high-speed train slipstream," *Journal of Wind Engineering and Industrial Aerodynamics*, vol. 165, pp. 46–57, Jun. 2017, doi: 10.1016/j.jweia.2017.03.001.
[19] S. Wang, J. R. Bell, D. Burton, A. H. Herbst, J. Sheridan, and M. C. Thompson, "The performance of different turbulence models (URANS, SAS and DES) for predicting high-speed train slipstream," *Journal of Wind Engineering and Industrial Aerodynamics*, vol. 165, pp. 46–53, 2017.
[20] S. Maleki, D. Burton, and M. C. Thompson, "Assessment of various turbulence models (ELES, SAS, URANS and RANS) for predicting the aerodynamics of freight train container wagons," *Journal of Wind Engineering and Industrial Aerodynamics*, vol. 170, pp. 68–80, Nov. 2017, doi: 10.1016/j.jweia.2017.07.008.
[21] E. Principe, *Il Veicolo Ferroviario*. Roma: Collegio Ingegneri Ferroviari Italiani, 2010.

[22] C. Baker *et al.*, *Train Aerodynamics: Fundamentals and Applications*. Cambridge: Butterworth-Heinemann, 2019.
[23] J. Östh and S. Krajnović, "A study of the aerodynamics of a generic container freight wagon using Large-Eddy Simulation," *J Fluids Struct*, vol. 44, pp. 31–51, Jan. 2014, doi: 10.1016/j.jfluidstructs.2013.09.017.